ACS Catalysis

Research Article

pubs.acs.org/acscatalysis

High-Pressure In Situ NMR Methods for the Study of Reaction Kinetics in Homogeneous Catalysis

Alexandre Torres,[†] Nieves Molina Perez,[†] Gillian Overend,[†] Nicholas Hodge,[†] Brian T. Heaton,[†] Jonathan A. Iggo,*[,†] John Satherley,[†] Robin Whyman,[†] Graham R. Eastham,[‡] and Darren Gobby[‡]

[†]Department of Chemistry, University of Liverpool, L69 7ZD Liverpool, United Kingdom, and

[‡]Lucite International, The Wilton Centre, Wilton, Redcar, TS10 4RF, United Kingdom.

Supporting Information

ABSTRACT: High-pressure NMR methods for the study of the kinetics of gas−solution reactions are presented, and the importance/interplay of mass transport and chemical resistances are discussed. For reactions that are slow compared with mass transport, the true reaction kinetics can be obtained and used to confirm that the observed species are relevant to the catalytic reaction. Conversely, the ability to determine the catalyst speciation during the catalytic reaction aids interpretation of the kinetic data. When chemical reaction is fast compared with diffusion across the gas−liquid interface, reaction is shown to occur in the liquid layer; for such a transport-controlled reaction, chemical reaction can increase the concentration gradient across the boundary layer, enhancing diffusion both across the phase boundary and within the liquid layer, resulting in apparent positive orders in catalyst, substrate, or both. These dependencies do not reflect the chemical dependence of the reaction rate on these concentrations.

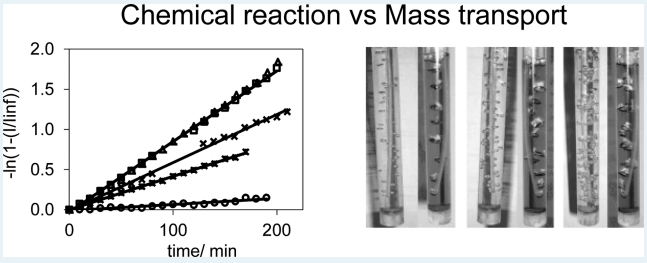

KEYWORDS: *high-pressure NMR, kinetics, hydroformylation, hydroesterification, methoxycarbonylation*

INTRODUCTION

HPNMR spectroscopy as a tool for mechanistic studies of organometallic, homogeneous catalysis[1] was introduced in the early 1980s by Heaton, Eguchi, and Jonas[2,3] and by Roe.[4−6] The two groups adopted different approaches: on the basis of earlier designs of Jonas intended for high pressure NMR studies of proteins, Heaton effectively built an NMR probe inside a nonmagnetic titanium alloy vessel;[7] Roe used a sapphire single crystal as an NMR tube, a titanium valve being glued to the open end of the tube.[6] Roe's design was popularized by Horvath,[8−10] Elsevier,[11−13] and Bianchini and Oberhauser[14] and is more convenient for general use, provided suitable safety precautions against sudden failure of the pressurized tube are taken. However, efficient gas transport across the gas−liquid interface and its subsequent diffusion throughout the reaction mixture is inevitably problematic in a long, thin, unmixed sample of small cross-sectional area. Failure to ensure sufficiently fast gas delivery to the reaction can cause the reaction to divert into side reactions made dominant by gas starvation,[15,16] an issue elegantly discussed in an excellent review by Garland.[9] For example, Nozaki showed that in the palladium−BINAPHOS-catalyzed copolymerization of styrene with CO, the reaction quickly became starved of CO in an unmixed high pressure NMR tube, the acyl intermediate disappearing from the ^{31}P NMR spectrum and additional decomposition pathways being observed.[17] Heaton and Jonas had recognized this problem in their pioneering studies and had used extreme overpressures of gas (up to 700 bar),[2,3] and Jonas developed a mechanically mixed version of the cell in an effort to deliver a sufficient quantity of gas to the reacting solution.[18]

Indeed, there is no a priori reason to believe that the species present in a HPNMR—indeed, in any—spectroscopic experiment must be the same as those present under reaction conditions.[19] We have, therefore, been interested for several years in the possibility of combining a kinetic study with in situ NMR characterization *in the same experiment* to establish a direct link between the catalysis (via the kinetics) and the NMR detected species. Conversely, knowledge of the species present in the reacting solution may aid the interpretation of kinetic data that might otherwise rely on assumptions about, for example, the rate-determining step, which, if incorrect, can lead to erroneous conclusions. Kinetic studies of all but the slowest reactions involving a gaseous reagent are self-evidently precluded in an unmixed NMR tube because it is essential that vapor liquid equilibrium is maintained; it is the solution concentration of the gas, not just the overpressure of gas present, that must equate to process conditions.[20,21] James and Fryzuk recognized and demonstrated this problem in their early HPNMR study of imine hydrogenation catalyzed by rhodium(I) phosphine

Special Issue: Operando and In Situ Studies of Catalysis

Received: July 4, 2012
Revised: September 14, 2012
Published: September 17, 2012

   dx.doi.org/10.1021/cs300439n | *ACS Catal.* 2012, 2, 2281−2289

complexes, concluding that kinetic studies of their system were not possible in an unmixed sapphire NMR tube.[22]

In this paper, we describe methods to address the mass transport problem and our high-pressure in situ NMR studies of two reactions: alkene hydroformylation and ethene methoxycarbonylation/hydroesterification (the Lucite ALPHA process) that illustrate the potential and limitations of the technique.

Alkene hydroformylation provides a good test case because it is known to be extremely sensitive to reaction conditions[23] and reaction occurs at a convenient rate for NMR study.[24−26] Moreover, a pre-equilibrium exists between dimers and monomers that is sensitive to hydrogen, CO, phosphorus ligand, and metal concentrations and in which the dimers are believed to represent an inactive catalyst reservoir (Scheme 1). It

Scheme 1. Catalytic Cycle for Rh−PR_3 Catalyzed Alkene Hydroformylation (linear product cycle shown)

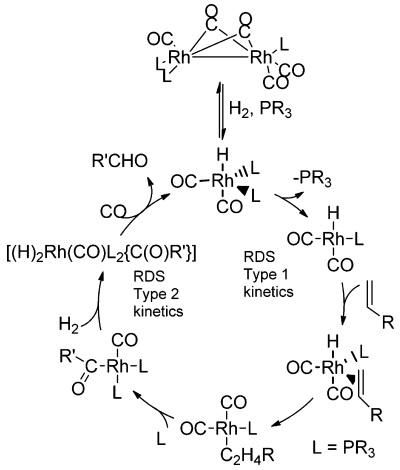

cannot, therefore, be assumed that the amount of catalytically active metal species present will be equal to the amount of rhodium precursor added to the reactor. In autoclave experiments, it is thus first necessary to establish that the reaction under study is first-order in rhodium catalyst precursor. If this is found not to be the case, then the metal added to the reactor will be partitioned between active monomer and inactive dimer. Furthermore, the position of the monomer−dimer equilibrium will change with pCO, pH_2, and the [phosphorus ligand]. In other words, the concentration of active Rh species in the autoclave cannot be known and will not be constant between experiments, even if the same amount of metal precursor is added to the reactor, complicating analysis of the kinetics. In contrast, in an in situ NMR kinetic experiment, the Rh speciation can be determined directly; hence, this problem does not arise.

Palladium-diphosphine-catalyzed methoxycarbonylation, on the other hand, is an extremely fast reaction and is included here because we were interested to discover what information about the catalyst performance/reaction regime might be obtained from an in situ high-pressure NMR study in such a case.

INSTRUMENTATION

Two high-pressure NMR cells were used in this work. The first is a refinement of our earlier design of a bubble column reactor[16] and is shown in Figure 1; the second is a modification of the dip tube/gas recirculation system developed by Baumann and Selent.[27,28]

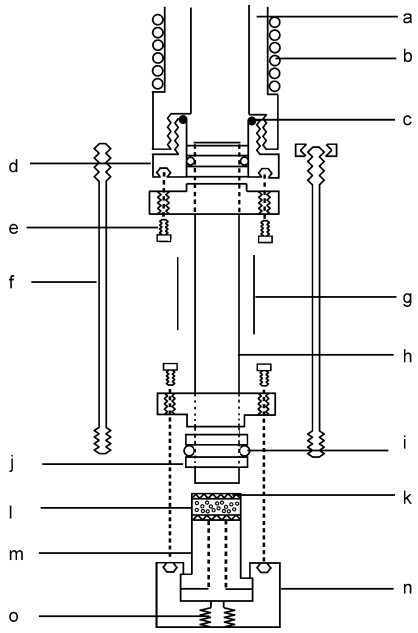

Figure 1. Exploded view of the HPNMR bubble column reactor: (a) top connection to gas outlet pipe, (b) 1/8 in. copper condenser tubing, (c) O-ring, (d) probe upper flange, (e) TiAlV6-4 cap-screw, (f) TiAlV6-4 tie bar, (g) NMR coil, (h) sapphire tube, (i) O-ring, (j) PTFE backup ring, (k) frit or PTFE gauze, (l) glass beads, (m) PTFE insert, (n) probe lower flange, and (o) 1/16 in. Swagelok seal.

The skeleton of the high-pressure, high-resolution bubble column provides support and protection against mechanical damage for the sapphire tube and is similar in design to that previously reported; however, the sealing arrangements have been significantly revised. In the new design, the pressure seals are compressed by a flange and tightened by three M4 machine screws (e) in place of the knurled nut previously used, which had been found to loosen on repeated temperature cycling of the HPNMR bubble column. The revised arrangement also removes one sealing surface compared with the old design, further improving performance. Finally, the new design allows removal of the sapphire tube without complete disassembly of the HPNMR probe. As in the previous design, a home-wound saddle coil (20 × 12.5 mm) is mounted directly around the sapphire tube and is tuned for X-nuclei. A second, free-standing coil (30 × 19 mm) is used for ^{1}H observe/decouple. Alternatively, the inner coil can be optimized for observation of nuclei in the range ^{19}F−^{1}H.

The HPNMR bubble column is mounted on a dural disk that bolts to the probe base. In the present design, a Bruker wide-bore NMR probe base is used. The proprietary rf tuning circuits incorporated in the commercial NMR probe base require retuning to accommodate the additional inductance of the longer coil tails, but this is readily achieved. Exceptionally, the ^{1}H tuning circuit must be moved to the dural mounting disk to further reduce the effect of this inductance. In principle, it should be possible to mount the bubble column on probe bases from any manufacturer, provided suitable mounting points exist.

The assembled HPNMR bubble column/probe is then contained within the outer sleeve of the commercial probe, providing a measure of protection to the user and protecting the sapphire tube from mechanical abrasion.[29]

The temperature of the sample is monitored by a PTFE sheathed T-type thermocouple inserted through the top of the

dx.doi.org/10.1021/cs300439n | ACS Catal. 2012, 2, 2281−2289

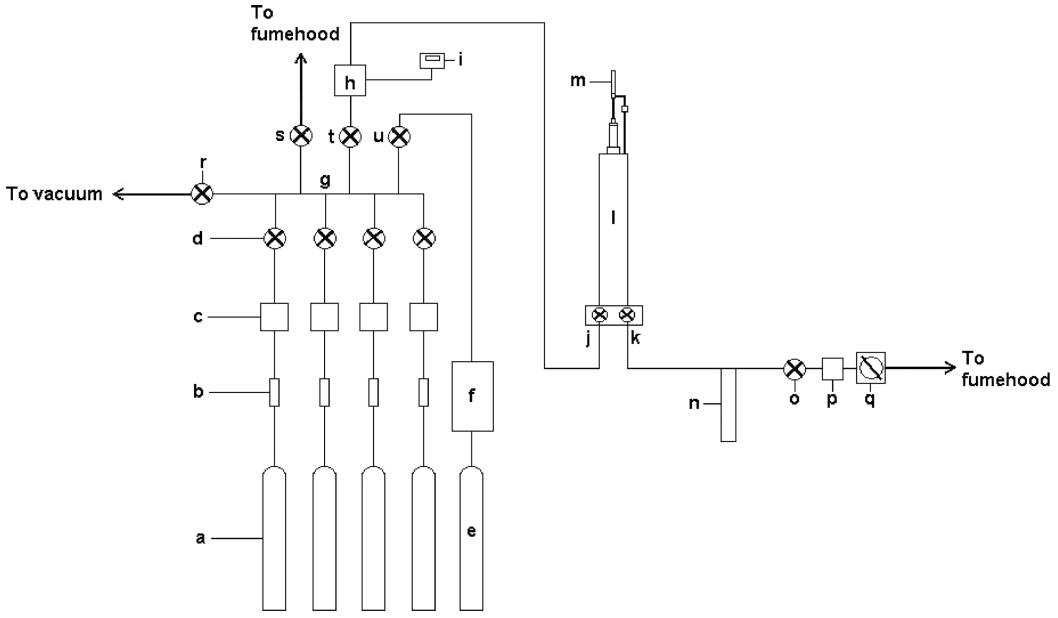

Figure 2. Schematic diagram of flow system: (a) gas cylinders, for example, CO, N_2, H_2 and ethylene; (b) Swagelok particulate filter (2 nm); (c) Brooks mass flow controller; (d) HiP valve; (e) CO_2 cylinder; (f) syringe pump; (g) manifold; (h) Druck pressure transducer; (i) digital pressure readout; (j) inlet HiP valve; (k) outlet HiP valve; (l) bubble column; (m) thermocouple; (n) cold trap; (o) HiP valve; (p) outlet mass flow controller; (q) back-pressure regulator; (r) HiP valve to vacuum line; (s) exhaust HiP valve; (t) master HiP valve; and (u) HiP valve.

probe via a Swagelok connector and is in direct contact with the reaction solution/sample. Heating and cooling of the sample is controlled using a Bruker VT 3200 unit. Sample temperatures can be maintained over the temperature range 233−493 ± 1 K, the accessible temperature range being limited by the elastomer O-rings.

Figure 2 shows a schematic of the gas delivery system used in the hydroformylation experiments.

A multiple gas feed scheme is used, with each gas (e.g., CO, H_2, ethylene and N_2) individually controlled using Brooks mass flow controllers (c) (operating range 0−60 L_n h^{-1}, typical flow rate under pressure is 20 L_n h^{-1}) allowing the composition of the inlet gas to be essentially infinitely varied. System pressure is controlled by balancing the inlet flow rates against that through a mass flow controller (p) and back pressure regulator (q). The gas travels along 1/8 in. stainless steel tubing from the gas cylinders, through Swagelok particulate filters (2 nm) (b) to the mass flow controllers (c), with all lines converging at a manifold (g). Additional connections to the manifold allow venting gases from the gas delivery system and connection to a vacuum line, which is used to purge the system of air prior to an experiment. A master HIP valve isolates the manifold from the bubble column. A Druck pressure transducer (h), mounted downstream of the master control valve monitors the pressure inside the HPNMR system. From thence, gas is fed to the HPNMR probe via a short length of 1/8 in. PEEK capillary tubing. A short length of 1/8 in. 316 stainless steel tubing is used to take gases from the base of the HPNMR probe to the base of the bubble column.[30] The dead volume of the system to this point is 15 mL. Gases then flow up through the bubble column and are returned to the base of the HPNMR probe via a return loop (1/16 in. Hastelloy C276 tubing) before passing through a cold trap to prevent any entrained solvent vapor from contaminating the outlet mass flow controller/back-pressure regulator. Finally, the outlet gases exhaust into a fume cupboard.

In the methoxycarbonylation experiments, in which isotopically labeled gases were used, a recirculating gas flow system (HiT GmbH, Rostock) was used.

RESULTS AND DISCUSSION

Several methods have been proposed to address mixing of gases into the solution in high-pressure NMR experiments, including mechanical stirring,[18,31] agitation by an oscillating magnetic field,[32] thermal convection currents within the sample, dip tubes/gas circulation devices,[33−35] bubble cells,[27,28] and bubble columns,[16] all of which can improve gas dissolution in comparison with a static Roe sapphire tube. Flow systems, such as our bubble column,[16] bring the added advantage of being able quickly to change the gas composition within the high-pressure NMR experiment without otherwise disturbing the sample. For example, Figure 3 compares the response of the hydrogen concentration dissolved in $CDCl_3$ at 65 bar pressure to changes in gas composition from a mixed N_2/H_2 gas stream in the bubble column with that of a sample contained within an NMR tube insert mimicking the conditions in a sapphire tube. VLE is achieved in <3 min in the bubble column, whereas in the latter, VLE is not achieved after 3000 min.

Alkene Hydroformylation; Intermediate Reaction Rate. The importance of considering mass transport in high-pressure NMR kinetic studies is underlined by the data in Figure 4, which shows reaction profiles for the rhodium-PBu^n_3-catalyzed hydroformylation of 1-hexadecene as a function of gas delivery *into* the reaction solution. An order of magnitude increase in reaction rate is seen as the flow rate is increased from 0 L_n h^{-1} (diffusion control) to 10 L_n h^{-1}. No further increase in the rate is observed on increasing the flow rate to 20 L_n h^{-1}, indicating that, above 10 L_n h^{-1}, the reaction rate is no longer limited by gas delivery, establishing the minimum gas flow rates required to maintain the reaction rate in the study below. The ^1H HPNMR spectra (see ESI) confirm that at these higher gas

dx.doi.org/10.1021/cs300439n | *ACS Catal.* 2012, 2, 2281−2289

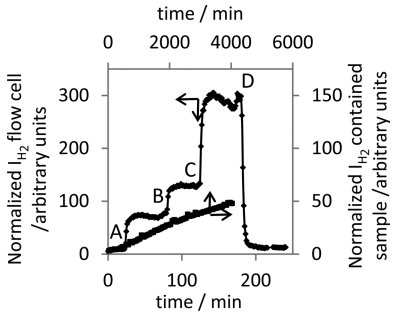

Figure 3. Evolution with time of the NMR intensity of the dissolved H_2 resonance during the dissolution of H_2 into 2.5% $CHCl_3$ in $CDCl_3$ at 290 K, 65 bar pressure. H_2/N_2 1:99; point A ratio of gases changed to H_2/N_2 1:4; point B, 1:1; point C, 4:1; point D, 1:99. The slight fall in relative intensity at 165 min reflects a slight, transient depressurization of the HPNMR cell at this point. The lower trace shows the evolution with time of the NMR intensity of the dissolved H_2 resonance during diffusion controlled uptake of H_2 from H_2/N_2 (4:1) into the same solvent mixture at the same temperature and pressure.

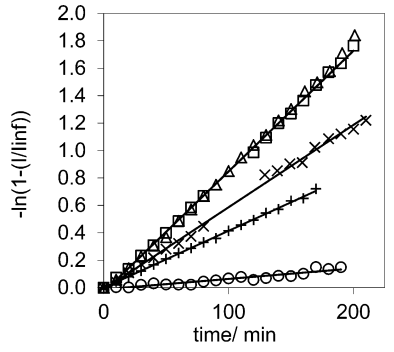

Figure 4. Rate of 1-hexadecene hydroformylation vs gas flow rate: ○, 0; +, 2; ×, 5; □, 10; Δ, 20 L_n h^{-1}. Conditions: 323 K; 45 bar CO/H_2, 1:1; [Rh] = 12.5 mM; [PBu^n_3], 25.8 mM; Rh/alkene, 1:68.

flow rates, the dissolved hydrogen gas is not depleted by reaction.

Two kinetic regimes are encountered in alkene hydroformylation (Scheme 1). In type 1 kinetics, the reaction shows positive orders in [alkene] and [rhodium] and negative orders in [ligand] and pCO, but is zero order in pH_2, which is consistent with the rate-determining step occurring early in the catalytic cycle, that is, is one of ligand dissociation, alkene coordination or insertion of the alkene into the Rh−H bond. Less commonly, the rate-determining step occurs late in the catalytic cycle, and a positive order in pH_2 and zero order in [alkene] is observed, type 2 kinetics.[23]

The reactions studied here were found to be first-order in alkene (see the Supporting Information), and [$HRh(CO)_2(PBu^n_3)_2$] was observed by in situ HPNMR as the catalyst resting state, irrespective of the alkene used (see the Supporting Information). Both observations are consistent with these catalytic systems obeying type 1 kinetics. The resting state is stable only under an atmosphere of CO/H_2 and was characterized as [$HRh(CO)_2(PBu^n_3)_2$] by ^1H, $^{31}P\{^1H\}$ HPNMR, and HPIR spectroscopy. Thus, a doublet of triplets attributable to a Rh-hydride is seen at $\delta_H = -9.9$ (dt, $^1J(RhH)$ = 8.1 Hz, $^2J(PH)$ = 16.4 Hz), which collapses to a doublet on ^{31}P decoupling, which is consistent with the presence of two phosphine ligands in the complex. The IR spectrum in the carbonyl region is complicated by the presence of dimeric species (vide infra), bands being seen at 2000(s), 1962(vs), 1778(s), and 1753(vs) cm^{-1};[36] however, an initial kinetic study of the effect of pH_2 on the reaction indicated a positive order in hydrogen consistent with type 2 kinetics (see the Supporting Information).

The in situ $^{31}P\{^1H\}$ NMR spectra also revealed the presence of dimers and the monomer (Figure 5) as well as small amounts

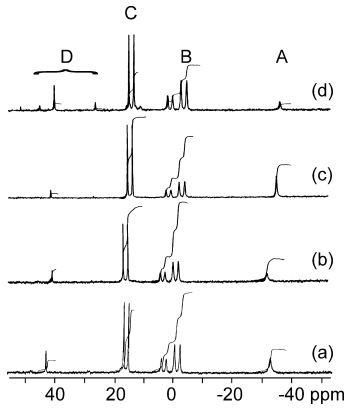

Figure 5. In situ $^{31}P\{^1H\}$ HPNMR spectra recorded during the hydroformylation of 1-decene. H_2 flow rate: (a) 5, (b) 7.5, (c) 10, and (d) 12.5 L_n h^{-1}. Conditions: 323 K; 45 bar; total gas flow rate, 20 L_n h^{-1}; CO flow rate, 7.5 L_n h^{-1}; N_2 balance. [Rh] = 14 mM, [PBu^n_3] = 28 mM, Rh/1-decene 1:67. A = PBu^n_3, B = [$Rh_2(CO)_5(PBu^n_3)_3$], C = [$HRh(CO)_2(PBu^n_3)_2$], D = decomposition products of PBu^n_3.

of impurities arising from decomposition of the phosphine during sample preparation and transfer to the HPNMR bubble column, (the major impurity, $\delta_P \sim 41$ ppm, is probably $OP(Bu^n)_3$).[37]

The dimers can be assigned as [$Rh_2(CO)_{8-n}(PBu^n_3)_n$] ($n$ = 4, $\delta_P = -4.9$ ppm, AA′A″A‴XX′ system, $^1J(RhP)$ = 148 Hz, $^3J(RhP)$ = 12 Hz, $^2J(PP)$ = 40 Hz, $^4J(PP) = {}^4J(PP^1)$ = 8H, 4P; n = 3, δ_P = 3.9 ppm, dtd, $^1J(RhP)$ = 129.2 Hz, $^3J(RhP)$ = 6.5 Hz, $^4J(PP)$ = 12.5 Hz, 1P, $\delta_P = -0.5$ ppm, $^1J(RhP)$ = 150.4 Hz, $^3J(RhP)$ = 7.1 Hz, $^4J(PP)$ = 12.5 Hz, 2P) by analogy with the work of Brown.[38] The monomer−dimer equilibrium is known to be sensitive to the presence of free phosphine and the partial pressures of the gases, the possibility therefore exists that the apparent positive order in H_2 is actually due to redistribution of this pre-equilibrium in response to changes in, for example, the dissolved H_2 concentration and is not indicative of type 2 kinetics.

Assuming type 1 kinetics and constant [CO], a simplified rate equation for the reaction can be written as eq 1.

$$\nu = k_{obs}\frac{[HRh(PBu_3)_2(CO)_2]^n[alkene]}{[free\ PBu_3]^m} \quad (1)$$

Assuming the reaction is first-order in the observed rhodium hydride complex, a log−log plot of initial rate/[$HRh(CO)_2(PBu^n_3)_2$] vs [free PBu^n_3] should afford the order of reaction in free PBu^n_3. Conversely, a log−log plot of initial rate × [free PBu^n_3] vs [$HRh(CO)_2(PBu^n_3)_2$] should afford the order of reaction in [$HRh(CO)_2(PBu^n_3)_2$]. In a second series of experiments using 1-dodecene, the required concentrations were determined from the $^{31}P\{^1H\}$ NMR integrals; the T_1 relaxation rates of the various phosphorus containing species were determined and are closely similar under catalytic conditions (see the Supporting Information). Figure 6 shows

dx.doi.org/10.1021/cs300439n | ACS Catal. 2012, 2, 2281−2289

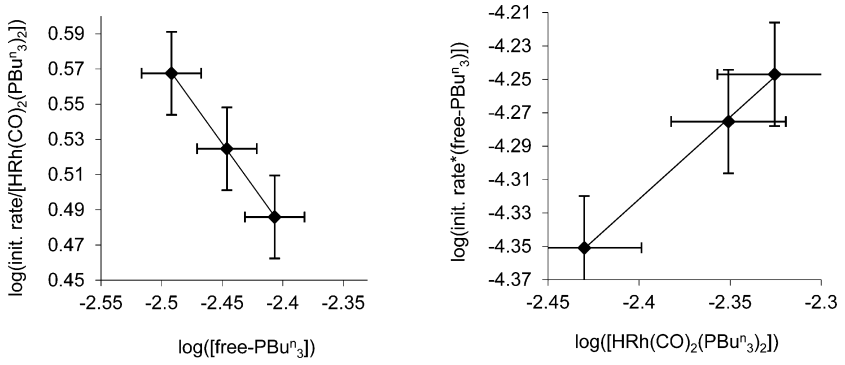

Figure 6. Log–log plots of initial rate/$[HRh(CO)_2(PBu^n_3)_2]$ vs [free PBu^n_3] and initial rate × [free PBu^n_3] vs $[HRh(CO)_2(PBu^n_3)_2]$ in the hydroformylation of 1-dodecene. Reaction conditions: 323 K, 45 bar $CO/H_2{:}N_2$. Flow rates: CO = 7.5 L_n h^{-1}, H_2 + N_2 = 12.5 L_n h^{-1}. [Rh] = 7.9 mM, [PBu^n_3] = 18.1 mM, Rh/1-dodecene 1:200.

the log–log plots of the initial rate data in this form, giving straight line plots of slope +0.98 for the order in $[HRh(CO)_2(PBu^n_3)_2]$ and −0.96 for the order in free PBu^n_3. A self-consistent picture then emerges of a reaction showing type 1 kinetics, that is, first order in *active* catalyst and alkene, shows first-order inhibition in free ligand, and is zero order in hydrogen. The rate-determining step occurs early in the catalytic cycle and either directly involves loss of phosphine from the catalyst resting state or ligand dissociation and is a necessary pre-equilibrium to the RDS. The concentrations of active species and free ligand required for this kinetic analysis are accessible only through the ability to monitor the speciation of the catalyst in situ during the catalytic reaction. The nature of the species involved in a catalytic process cannot always be straightforwardly determined by NMR spectroscopy, either because they are present in too low a concentration or have to short a lifetime to be detected by NMR. The possibility thus exists that the spectroscopically detected species are not involved in the catalysis. The in situ NMR methodology inherently monitors catalyst stability/decomposition, and the kinetic analysis confirms that the species observed here, $[HRh(CO)_2(PBu^n_3)_2]$, is directly involved in the catalytic cycle.

Alkene Methoxycarbonylation; High Reaction Rate. Stage 1 of the recently introduced Lucite ALPHA process employs Pd-diphosphine-catalyzed methoxycarbonylation of ethene to methyl propanoate, which in a separate, heterogeneous base-catalyzed step is subsequently reacted with formaldehyde to give methyl methacrylate (Scheme 2).[39−46] The first commercial scale plant came on stream in 2008[47] and produces 140 ktons p.a. of MMA, the palladium-diphosphine catalyst used affording high reaction rates around 50 000 h^{-1}.[39] We expected this fast reaction to show mass transfer effects and therefore investigated the effect of mixing and interfacial surface area on the observed reaction rate.

No standing concentration of carbon monoxide was observed in the liquid bulk in preliminary reactions performed using a gas flow rate of 12 $mLmin^{-1}$ and a simple PTFE dip tube to deliver gas to the reaction, which is consistent with slow mass transfer compared with the reaction rate, that is, carbon monoxide is consumed so rapidly by the reaction that it does not reach the bulk of the liquid phase. Under these conditions of slow mass transfer, reaction occurs in the liquid film surrounding the gas bubbles. The mass transfer rate can be increased by increasing the contact surface between phases, for example, by increasing the gas flow rate, reducing the bubble size, or both. Increasing the gas flow rate to 30 $mLmin^{-1}$ results in a very turbulent

Scheme 2. Lucite ALPHA Process for Production of Methyl Methacrylate[a]

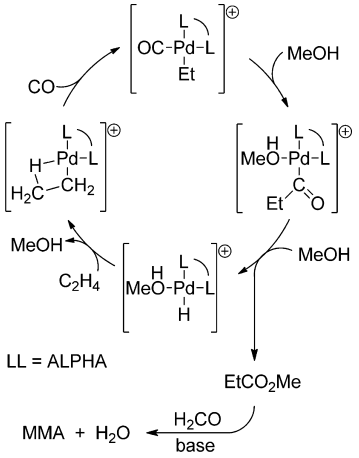

[a]Stage 1 converts ethene, CO, and MeOH into methyl propanoate (MeP); stage 2 transforms MeP into methyl methacrylate by reaction with formaldehyde.

system in which entrained liquid is carried out of the reaction cell, and the resolution in the NMR spectra is severely degraded. We therefore modified the gas delivery tube to reduce the bubble size. An open-ended tube delivers large gas bubbles (~6 mm diameter). In contrast, a tube with a sealed end and perforated by two small holes placed diametrically opposite at the bottom of the tube delivers smaller bubbles (~3.2 mm diameter) with little coalescence of the bubbles observed as these travel up through the solution to the top of the reaction cell. The change in the contact surface area between gas and liquid with gas flow rate and bubble size is evident in Figure 7, which shows pictures of the reaction bubble cell at flow rates of 20, 30, and 40 mL/min using the original (right) and modified (left) gas delivery tube.

Two reactions were then performed at a gas flow rate of 30 $mLmin^{-1}$, the first using the original delivery tube, that is, with large gas bubbles, and a second otherwise identical reaction but using the modified tube, that is, with small bubbles. The contact surface area between gas and liquid was determined by measuring the average diameter of the bubbles and counting the number of bubbles in the reaction cell; the contact area between phases was found to be 1.1×10^{-3} m^2, and 1.9×10^{-3} m^2 respectively. As mentioned above, in the experiment using the unmodified dip tube, no carbon monoxide dissolved in the

dx.doi.org/10.1021/cs300439n | ACS Catal. 2012, 2, 2281−2289

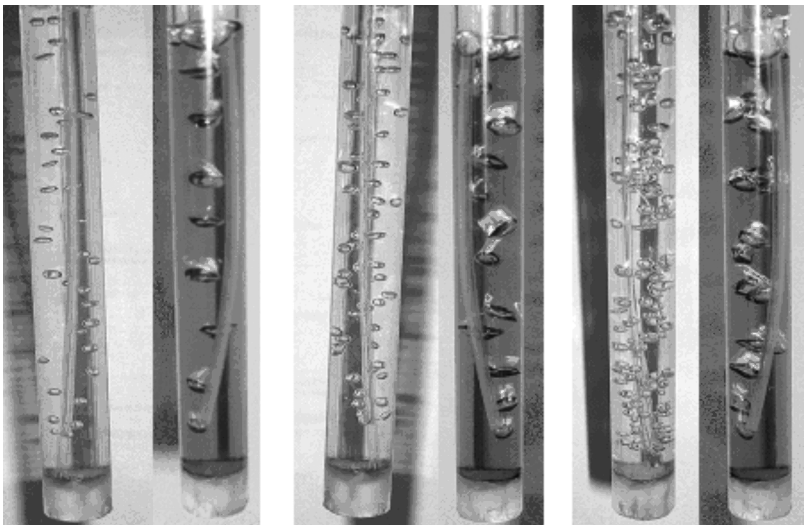

Figure 7. Effect of bubble size and gas flow rate on interfacial contact area. In each pair of images, the left image shows the modified dip tube. Gas flow rates are (left) 20, (center) 30, and (right) 40 mL min^{-1}.

liquid bulk was detected; however, when the modified tube giving smaller bubbles was used, a very low concentration of dissolved CO was observed at the beginning of the reaction, but this disappeared quickly. As expected, using the modified tube, the initial rates increased in the second reaction from 2.51×10^{-3} mol (MeP) h^{-1}, to 5.29×10^{-3} mol (MeP) h^{-1}; that is, the reaction rate is limited by mass transfer effects as a result of a high reaction rate with respect to mass transport.

A full kinetic analysis of mass transport controlled reactions occurring in the boundary layer is complex[48,49] and has been reviewed by Middleton.[50] Nonetheless, it is possible to determine the reaction regime[50] by observing how variation of mass transfer, composition of the gas stream, and palladium concentration affect the observed rate. Four possible reaction regimes must be considered in these experiments, classified by Middleton[50] as (II) moderately fast reaction, (III) fast reaction, (IV) very fast reaction, or (V) instantaneous reaction (Table 1).

Table 1. Classification of Reaction Regimes for Gas-Solution Reactions Made by Middleton

	regime	characteristics
I	slow reaction	kinetic control
II	moderately fast reaction in bulk of the liquid	diffusion of dissolved species controls rate
III	fast reaction in the film	pseudo-first-order in species dissolving from the gas phase into the liquid; $C_{MeOHbulk} >>> C_{COinterface}$; $C_{CObulk} = 0$
IV	very fast reaction	general case of III; $C_{MeOHbulk} \sim C_{COinterface}$; $C_{CObulk} = 0$
V	instantaneous reaction	reaction at interface, rate controlled by diffusion of dissolved substrate from bulk to interface

Regime I, the slow reaction, in which the chemical reaction rate controls the overall rate, is not relevant to this mass-transport-controlled system. When the chemical reaction rate is moderately faster than mass transport, the overall rate will be mass-transfer-controlled (regime II). However, for very fast reactions in the liquid film, regimes III and IV, the chemical reaction itself can enhance the diffusion process because consumption of the diffusing gas by the reaction increases the concentration gradient in the boundary layer—the concentration of CO in the gas phase in the bubble reactor is essentially constant—increasing the mass transfer rate above the purely physical rate. The extent of this enhancement will be a function of the chemical reaction rate and thus will be influenced by the concentration of (other) dissolved reactants as well as the concentration of the dissolving species.[50] In the limit of extremely fast reaction, mass transfer again controls the overall rate, and the reaction rate is no longer affected by the concentration of a reagent, regime V, instantaneous reaction.

A linear relationship between reaction rate and contact area between phases is observed on changing the gas feed flow rate and, hence, interfacial area (Figure 8), confirming our initial conclusion that the reaction rate is mass-transport-controlled and occurs in the liquid film.

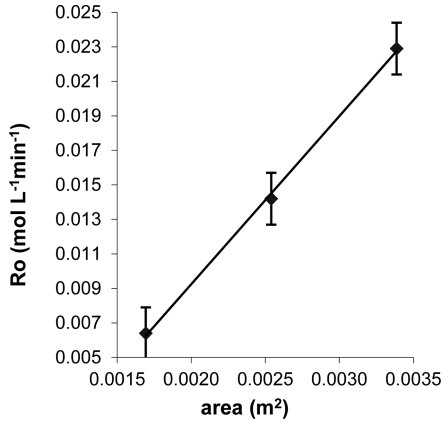

Figure 8. Effect of variation in interfacial area as a result of changing gas flow rate 20, 30, 40 mL/min. pCO 1.2 bar, 8.2 M methanol, and 5 ppm Pd.

The linear relationship observed between the concentration of CO in the liquid film—CO is the limiting gaseous component due to its lower solubility in the reaction medium—and the reaction rate on varying the partial pressure of CO in the gas phase (Figure 9) eliminates an instantaneous reaction (regime V) but is consistent with regimes III or IV.

dx.doi.org/10.1021/cs300439n | ACS Catal. 2012, 2, 2281−2289

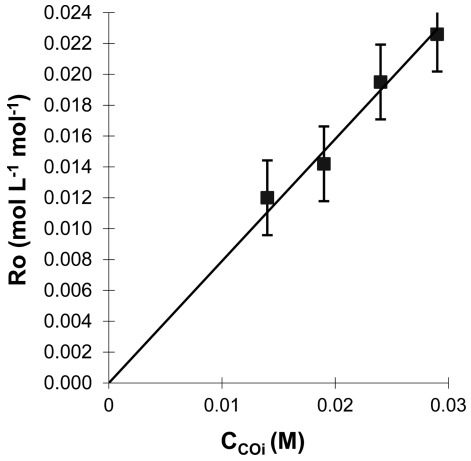

Figure 9. Effect of carbon monoxide film concentration[51] on reaction rate. Gas flow rate, 30 mL min^{-1}; 8.2 M methanol; small bubble size; and 5 ppm palladium.

As discussed above, for these fast, diffusion-controlled reaction regimes, the observed rate is determined by mass transport, not by the chemical rate. The reaction, however, can still show a rate dependence on catalyst concentration (Figure 10) because the greater the concentration of palladium, the more active centers are present. This results in faster depletion of CO from the boundary layer where reaction is taking place, increasing the concentration gradient and, hence, increasing the mass transport rate. Because the reaction is known to be limited by mass transport (Figure 8), the observed increase in reaction rate (Figure 10) must reflect an enhanced mass transport rate resulting from an increase in the CO concentration gradient as a consequence of chemical reaction. Although palladium-catalyzed hydroesterification reactions have been reported previously to be first-order in [Pd][52] and stage 1 of the Lucite ALPHA is known also to be first-order in [Pd],[53] the linear relationship evident in Figure 10 between [Pd] and the reaction rate in this mass-transport-controlled reaction must reflect mass transport phenomena rather than the true dependence of the rate on [Pd].

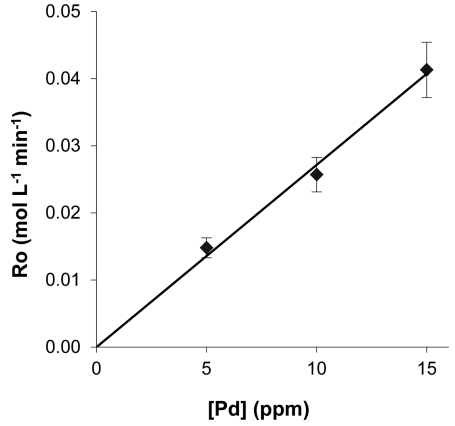

Figure 10. Effect of [Pd] on the observed initial rate of reaction. Gas flow rate, 30 mL min^{-1} 8.2 M methanol; small bubble size; and 5–15 ppm palladium.

For each reaction, the mass transfer rate can be estimated by applying a mass balance to carbon monoxide (the quantity of carbon monoxide transferred from the gas phase to the liquid phase must equal the quantity of CO consumed in the reaction plus the quantity of CO dissolved in the liquid bulk) and an apparent mass transfer coefficient, k_{Lobs}, obtained using the interfacial area determined above (Figure 11). Faster mass transfer occurs with increasing reaction rate; the CO transferred from the gas phase is consumed rapidly; thus, the CO concentration gradient through the liquid film is high at all times, resulting in an increased rate of mass transfer. Because the concentration of CO in the liquid film is much lower than the concentration of methanol in the reaction medium, we can conclude that the reaction regime pertaining in the sapphire tube in this gas–liquid reaction is III, that is, fast pseudo-first-order in CO, and reaction occurs in the liquid film.

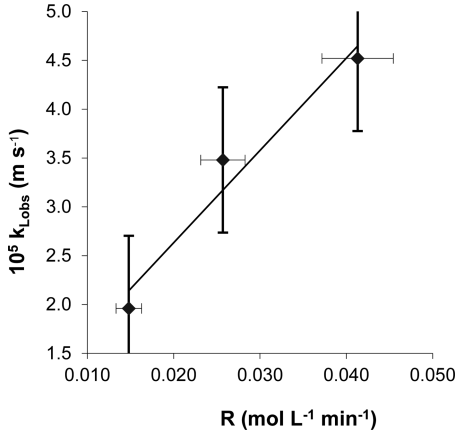

Figure 11. Mass transfer coefficient as a function of reaction rate.

CONCLUSIONS

When reaction occurs in the liquid phase, two distinct physical phenomena (interfacial mass transfer between gas and liquid) and reaction in the liquid phase occur simultaneously. Thus, in studies of the overall process rate, two different resistances, mass transport, and the resistance of the chemical reaction process must be considered. The relative values of these resistances will define the kinetic regime of the overall process. If the mass transfer process is very slow relative to the reaction, the overall process will be governed by the mass transfer step. On the other hand, in a slow chemical reaction with fast mass transfer, the overall rate observed will correspond to the chemical reaction rate. These two extreme cases are easily distinguished because the overall rate will reduce to one or the other single process, mass transfer or chemical reaction. However, in general, the behavior of gas–liquid reactions falls in an intermediate regime in which both mass transfer and chemical reaction resistances are significant. In that case, the reaction occurs at the interface as well as/instead of in the bulk of liquid. Hence, attention must be given to mass transfer between the gas and the liquid phase to understand the operating kinetic regime, as in the case of ethene methoxycarbonylation. Experimental design is, therefore, crucial in in situ HPNMR studies of reaction kinetics; effective mixing of gaseous reagents into solution must be ensured if meaningful kinetic data are to be obtained.

Care must also be taken in interpretation of the kinetic data. Where turnover frequencies are in the range of tens to hundreds per hour, as in the case of the alkene hydroformylation catalysis performed in the HPNMR bubble column and described above, the true reaction kinetics, unaffected by mass transport, can be observed and used to establish a direct link between the species

dx.doi.org/10.1021/cs300439n | ACS Catal. 2012, 2, 2281–2289

observed and the catalysis itself. Such studies are particularly useful in systems in which the amount of catalyst precursor added to the reaction does not correspond to the amount of active catalytic species present during the reaction because the speciation of the catalyst may be determined from the in situ HPNMR spectra. For reactions occurring at much faster rates, TOF ~ 10 000 h^{-1}, an apparent (reasonable) order in, for example, catalyst may in fact reflect mass transport phenomena, which may in turn be driven by the chemical reaction enhancing the concentration gradient in the interfacial liquid layer rather than a chemical rate dependence. Current HPNMR gas-mixing devices are not able to deliver sufficiently high mass transport rates to these very fast reactions; nevertheless, meaningful information about the kinetic regime can be obtained.

EXPERIMENTAL SECTION

All NMR measurements were performed on a Bruker AMX2-200WB spectrometer using home-built high-pressure NMR probes or in a sapphire tube in a commercial 10 mm probe. $[Pd_2(dba)_3]$, $Gd(MeSO_3)_3$, and 1,2-bis(di-*tert*-butylphosphinomethyl)benzene were donated by Lucite International. ^{13}CO was purchased from CK Gas Products Ltd., and ethene, CO, and nitrogen were from BOC. Alkenes and NMR solvents were purchased from Aldrich and dried over activated molecular sieves and degassed before use. PBu^n_3 was purchased from Strem and stored under nitrogen.

Alkene Hydroformylation. Stock solutions of $[Rh(acac)(CO)_2]$ and PBu^n_3 in degassed, N_2-saturated, toluene-d_8 were prepared by dissolving $[Rh(acac)(CO)_2]$ (77.4 mg, 0.3 mmol) or PBu^n_3 (170 μL, 0.688 mmol) in 12 mL of toluene-d_8 and stored under nitrogen. 1-Hexadecene, 1-dodecene, and 1-decene were used in the kinetic experiments because of the low volatility of both these substrates and the expected aldehyde products. In a typical experiment, 1.9 mL of each stock solution was mixed with 1−2 mL of alkene as required giving a Rh/PBu^n_3/alkene ratio of 1:2.29:67−191. The solution was transferred to the bubble column under nitrogen, the bubble column was sealed, and the reactor was purged with hydrogen. The sample was shimmed, then pressurized to the desired pressure with CO/H_2, gas ratio 4:1 to 1:4, as required, and the desired gas flow rate was set by the inlet mass flow controllers. N_2 was used as a ballast gas to maintain a constant total system pressure and gas flow rate in each experiment. A $^{31}P\{^1H\}$ NMR spectrum was then recorded. ^1H NMR spectroscopy revealed that no significant reaction had taken place. The sample was then heated rapidly (<4 min) to reaction temperature, typically 323 K. Temperature overshoot was limited to <2 K by careful adjustment of the heater power and heating gas flow rate. Temperature stability during reaction typically was ±1 K. ^1H NMR spectra were then recorded at 10 min intervals, the acquisition time was typically 2 min, and the total reaction time was typically 3 h. $^{31}P\{^1H\}$ spectra were recorded at the beginning, in the middle, and at the end of each experiment to determine the speciation of the ^{31}P-containing compounds present and to check for degradation of the sample during reaction. The integrated intensity of the aldehyde product was determined from the ^1H NMR spectra and fitted to a first-order exponential growth to obtain the rate constant.

Ethene Methoxycarbonylation. [(ALPHA)Pd(dba)] was prepared in situ by the addition of 1,2-bis(di-*tert*-butylphosphinomethyl)benzene (ALPHA) and $[Pd_2(dba)_3]$ (dba = *trans,trans*-dibenzylideneacetone) to a 6 g/L solution of $Gd(MeSO_3)_3$ in a mixture of methyl propanoate/methanol (70%, 30% mass composition). Methanesulfonic acid was then added to generate a complex capable of converting ethene, carbon monoxide, and methanol to methyl propanoate. The compositions of the catalyst species in the final reacting solution were [Pd] = 5−15 ppm, $[L_2]$ = 40−50 ppm, and $[MeSO_3H]$ = 2000 ppm. The reaction solution was prepared and kept under nitrogen due to the sensitivity of the catalyst complex to oxygen. Four milliliters of this solution was introduced, under nitrogen, into the reaction cell (consisting of a sapphire tube connected to the gas recirculation system described above). The system was then sealed, the liquid solution was frozen, and the apparatus was evacuated. The reaction cell and gas recirculation system were then pressurized to 15−20 bar with a mixture of ethene/^{13}CO [4:1 molar ratio]. The reaction gas was then pumped at a flow rate of 30 mL/min through the reaction solution. The reaction cell was then introduced into the NMR magnet, and the solution composition measurement was taken. Reaction was then initiated by raising the reactor temperature to 373 K. Gases consumed by the reaction were replenished from a ballast cylinder containing a mixture of ethene/^{13}CO [1:1 molar ratio] via a forward pressure regulator so that the composition of the gas phase and the total pressure of the system was constant. The composition of the reacting solution was monitored with time by $^{13}C\{^1H\}$ NMR. Figure 12 presents the $^{13}C\{^1H\}$NMR spectra recorded during a typical reaction.

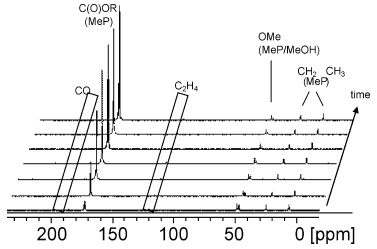

Figure 12. Stack plot of the $^{13}C\{^1H\}$ NMR spectra showing the time course of a typical reaction recorded over 3 h.

ASSOCIATED CONTENT

Supporting Information

T_1 relaxation measurements and representative HPNMR spectra and kinetic fits. This material is available free of charge via the Internet at http://pubs.acs.org/.

AUTHOR INFORMATION

Corresponding Author

*Email iggo@liverpool.ac.uk.

Notes

The authors declare no competing financial interest.

ACKNOWLEDGMENTS

This work was supported by the Engineering and Physical Science Research Council [Grant No. EP/C005643/1]; Lucite International; and BP Chemicals (Hull). We thank Drs. A. Poole, G. Morris, D. Taylor, D. Law, and R. Watt (BP Chemicals) for helpful discussions.

ABBREVIATIONS

HPNMR, high pressure NMR Spectroscopy; MeP, methyl propanoate; dba, dibenzylideneacetone; acac, acetyl aceonate; Bu^n, normal butyl; ALPHA, 1,2-bis(di-*tert*-butylphosphinomethyl)benzene; BINAPHOS, (2-(diphenyl-

phosphino)-1,1′-binaphthalen-2′-yl)-(1,1′-binaphthalen-2,2′-yl)-phosphite; TiAlV6-4, titanium alloy containing 6% Al, 4% V; dural, aluminum/copper/magnesium alloy; L_n, normal liter, amount of pressurized gas that would occupy 1 L if at STP; HiP, High Pressure Equipment Company

REFERENCES

(1) Laurenczy, G.; Helm, L., High Pressure NMR Cells. In *Mechanisms in Homogeneous Catalysis − A Spectroscopic Approach*; Heaton, B. T., Ed.; Wiley-VCH Verlag GmbH & Co. KGaA: Weinheim, 2005; pp 81−106.
(2) Heaton, B. T.; Strona, L.; Jonas, J.; Eguchi, T.; Hoffman, G. A. *J. Chem. Soc., Dalton Trans.* **1982**, 1159−1164.
(3) Heaton, B. T.; Jonas, J.; Eguchi, T.; Hoffman, G. A. *J. Chem. Soc., Chem. Commun.* **1981**, 331−332.
(4) Roe, D. C.; Kating, P. M.; Krusic, P. J.; Smart, B. E. *Top. Catal* **1998**, *5*, 133−147.
(5) Roe, D. C. *Adv. Chem. Ser.* **1992**, 33−46.
(6) Roe, D. C. *J. Magn. Reson.* **1985**, *63*, 388−391.
(7) Defries, T. H.; Jonas, J. *J. Magn. Reson.* **1979**, *35*, 111−119.
(8) Csihony, S.; Mika, L. T.; Vlad, G.; Barta, K.; Mehnert, C. P.; Horvath, I. T. *Collect. Czech. Chem. Commun.* **2007**, *72*, 1094−1106.
(9) Garland, G. Transport Effects in Homogeneous Catalysis. In *The Encyclopedia of Catalysis*; Horvath, I. T., Ed.; John Wiley & Sons, Inc.: Hoboken, 2002; Vol. *6*, p 550.
(10) Horvath, I. T.; Millar, J. M. *Chem. Rev.* **1991**, *91*, 1339−1351.
(11) Leone, A.; Gischig, S.; Elsevier, C. J.; Consiglio, G. *J. Organomet. Chem.* **2007**, *692*, 2056−2063.
(12) Sprengers, J. W.; Kluwer, A. M.; Gaemers, S.; Elsevier, C. J., *High-Pressure NMR Spectroscopy: Some General Aspects and Applications*. **2002**; Vol. *208-2*, p 283−294.
(13) Elsevier, C. J. *J. Mol. Catal.* **1994**, *92*, 285−297.
(14) Rubio, M.; Suarez, A.; Alvarez, E.; Bianchini, C.; Oberhauser, W.; Peruzzini, M.; Pizzano, A. *Organometallics* **2007**, *26*, 6428−6436.
(15) Hamilton, R. J.; Leong, C. G.; Bigam, G.; Miskolzie, M.; Bergens, S. H. *J. Am. Chem. Soc.* **2005**, *127*, 4152−4153.
(16) Iggo, J. A.; Shirley, D.; Tong, N. C. *New J. Chem.* **1998**, *22*, 1043−1045.
(17) Iggo, J. A.; Kawashima, Y.; Liu, J.; Hiyama, T.; Nozaki, K. *Organometallics* **2003**, *22*, 5418−5422.
(18) Vandervelde, D. G.; Jonas, J. *J. Magn. Reson.* **1987**, *71*, 480−484.
(19) Landis, C. R.; Halpern, J. *J. Am. Chem. Soc.* **1987**, *109*, 1746−1754.
(20) Denney, M. C.; Smythe, N. A.; Cetto, K. L.; Kemp, R. A.; Goldberg, K. I. *J. Am. Chem. Soc.* **2006**, *128*, 2508−2509.
(21) Goldberg, K. I., Mechanistic Studies of Fundamental Reaction Steps in Late Metal Homogeneous Catalysis. In *XXI International Conference on Organometallic Chemistry*, Vancouver, July 25−30, 2004.
(22) Ball, G.; Cullen, W. R.; Fryzuk, M. D.; Henderson, W. J.; James, B. R.; MacFarlane, K. S. *Inorg. Chem.* **1994**, *33*, 1464−1468.
(23) van Leeuwen, P. W. N. M.; Claver, C., *Rhodium Catalyzed Hydroformylation*; Kluwer Academic Publishers: Dordrecht, 2000; Vol. *22*, pp 63−165.
(24) Nozaki, K.; Matsuo, T.; Shibahara, F.; Hiyama, T. *Organometallics* **2003**, *22*, 594−600.
(25) Chaudhari, R. V.; Seayad, A.; Jayasree, S. *Catal. Today* **2001**, *66*, 371−380.
(26) van der Slot, S. C.; Kamer, P. C. J.; van Leeuwen, P. W. M. N.; Iggo, J. A.; Heaton, B. T. *Organometallics* **2001**, *20*, 430−441.
(27) Selent, D.; Franke, R.; Kubis, C.; Spannenberg, A.; Baumann, W.; Kreidler, B.; Boerner, A. *Organometallics* **2011**, *30*, 4509−4514.
(28) Baumann, W.; Mansel, S.; Heller, D.; Borns, S. *Magn. Reson. Chem.* **1997**, *35*, 701−706.
(29) The actual, as opposed to theoretical, safe working pressure of high-pressure sapphire tubes is dependent on the history and condition of the tube. Tubes that are chipped or scratched, or have experienced temperature or pressure shocks have unknown safe working pressures, are liable to sudden catastrophic failure, and should be discarded.
(30) PEEK tubing was found not to be suitable for the gas line feeding the bubble column because some seepage of solvent through the frit is inevitable. PEEK was found to be incompatible with many of the solvents at the temperatures and pressures routinely used.
(31) Cusanelli, A.; Frey, U.; Marek, D.; Merbach, A. E. *Spectrosc. Eur.* **1997**, *9*, 22−27.
(32) Kramarz, K. W.; Klingler, R. J.; Fremgen, D. E.; Rathke, J. W. *Catal. Today* **1999**, *49*, 339−352.
(33) Woelk, K.; Bargon, J. *Rev. Sci. Instrum.* **1992**, *63*, 3307−3310.
(34) Niessen, H. G.; Trautner, P.; Wiemann, S.; Bargon, J.; Woelk, K. *Rev. Sci. Instrum.* **2002**, *73*, 1259−1266.
(35) Niessen, H. G.; Trautner, P.; Backhausen, R.; Woelk, K. *Concepts Magn. Reson., Part B* **2003**, *16B*, 15−21.
(36) Shirley, D. *The Development of a High Pressure In-Situ NMR Probe for the Study of Homogeneous Catalysis*, Ph.D. dissertation, The University of Liverpool, Liverpool, 1999.
(37) We thank a referee for this suggestion.
(38) Brown, D. T.; Eguchi, T.; Heaton, B. T.; Iggo, J. A.; Whyman, R. *J. Chem. Soc., Dalton Trans.* **1991**, 677−683.
(39) Clegg, W.; Eastham, G. R.; Elsegood, M. R. J.; Tooze, R. P.; Wang, X. L.; Whiston, K. *Chem. Commun.* **1999**, 1877−1878.
(40) Eastham, G. R.; Heaton, B. T.; Iggo, J. A.; Tooze, R. P.; Whyman, R.; Zacchini, S. *Chem. Commun.* **2000**, 609−610.
(41) Eastham, G. R.; Tooze, R. P.; Kilner, M.; Foster, D. F.; Cole-Hamilton, D. J. *J. Chem. Soc., Dalton Trans.* **2002**, 1613−1617.
(42) Knight, J. G.; Doherty, S.; Harriman, A.; Robins, E. G.; Betham, M.; Eastham, G. R.; Tooze, R. P.; Elsegood, M. R. J.; Champkin, P.; Clegg, W. *Organometallics* **2000**, *19*, 4957−4967.
(43) Clegg, W.; Eastham, G. R.; Elsegood, M. R. J.; Heaton, B. T.; Iggo, J. A.; Tooze, R. P.; Whyman, R.; Zacchini, S. *J. Chem. Soc., Dalton Trans.* **2002**, 3300−3308.
(44) Clegg, W.; Eastham, G. R.; Elsegood, M. R. J.; Heaton, B. T.; Iggo, J. A.; Tooze, R. P.; Whyman, R.; Zacchini, S. *Organometallics* **2002**, *21*, 1832−1840.
(45) Donald, S. M. A.; Macgregor, S. A.; Settels, V.; Cole-Hamilton, D. J.; Eastham, G. R. *Chem. Commun.* **2007**, 562−564.
(46) de la Fuente, V.; Waugh, M.; Eastham, G. R.; Iggo, J. A.; Castillon, S.; Claver, C. *Chem.—Eur. J.* **2010**, *16*, 6919−6932.
(47) http://www.luciteinternational.com/.
(48) Coulson, J. M.; Richardson, J. F. *Chemical Engineering*; Pergamon Press: London, 1971; Vol. *3*.
(49) Astarita, G. *Mass Transfer with Chemical Reaction*; Elsevier: New York, 1967.
(50) Middleton, J. C.; Harnby, N.; Nienow, A. W.; Edwards, M. F. Gas−liquid Dispersion and Mixing. In *Mixing in the Process Industries*, 2nd ed.; Butterworth-Heinemann: Oxford, 1997; pp 349−352.
(51) Torres, A. *In situ measurement of gas concentrations in working catalytic reactors by HPNMR*. PhD dissertation, University of Liverpool, Liverpool, 2009.
(52) Vavasori, A.; Toniolo, L.; Cavinato, G. *J. Mol. Catal. A: Chem.* **2003**, *191*, 9−21.
(53) Gavriilidis, A. Personal communication.